Sequence-Specific Transcription Factor NF-Y Displays Histone-like DNA Binding and H2B-like Ubiquitination

- Marco Nardini[1, 5], Nerina Gnesutta[1, 5], Giacomo Donati[1, 5], Raffaella Gatta[1], Claudia Forni[1], Andrea Fossati[1], Clemens Vonrhein[3], Dino Moras[4], Christophe Romier[4], Martino Bolognesi[1, 2,], Roberto Mantovani[1,]

- [1] Dipartimento di BioScienze, Università degli Studi di Milano, Via Celoria 26, 20133 Milano, Italy
- [2] CNR, Istituto di Biofisica, and CIMAINA, Università degli Studi di Milano, Via Celoria 26, 20133 Milano, Italy
- [3] Global Phasing Ltd., Sheraton House, Castle Park, Cambridge CB3 0AX, UK
- [4] Département de Biologie et Génomique Structurales, IGBMC, 67404 Illkirch Cedex, France
- [5] These authors contributed equally to this work

Show more

http://dx.doi.org/10.1016/j.cell.2012.11.047

Summary

The sequence-specific transcription factor NF-Y binds the CCAAT box, one of the sequence elements most frequently found in eukaryotic promoters. NF-Y is composed of the NF-YA and NF-YB/NF-YC subunits, the latter two hosting histone-fold domains (HFDs). The crystal structure of NF-Y bound to a 25 bp CCAAT oligonucleotide shows that the HFD dimer binds to the DNA sugar-phosphate backbone, mimicking the nucleosome H2A/H2B-DNA assembly. NF-YA both binds to NF-YB/NF-YC and inserts an α helix deeply into the DNA minor groove, providing sequence-specific contacts to the CCAAT box. Structural considerations and mutational data indicate that NF-YB ubiquitination at Lys138 precedes and is equivalent to H2B Lys120 monoubiquitination, important in transcriptional activation. Thus, NF-Y is a sequence-specific transcription factor with nucleosome-like properties of nonspecific DNA binding and helps establish permissive chromatin modifications at CCAAT promoters. Our findings suggest that other HFD-containing proteins may function in similar ways.

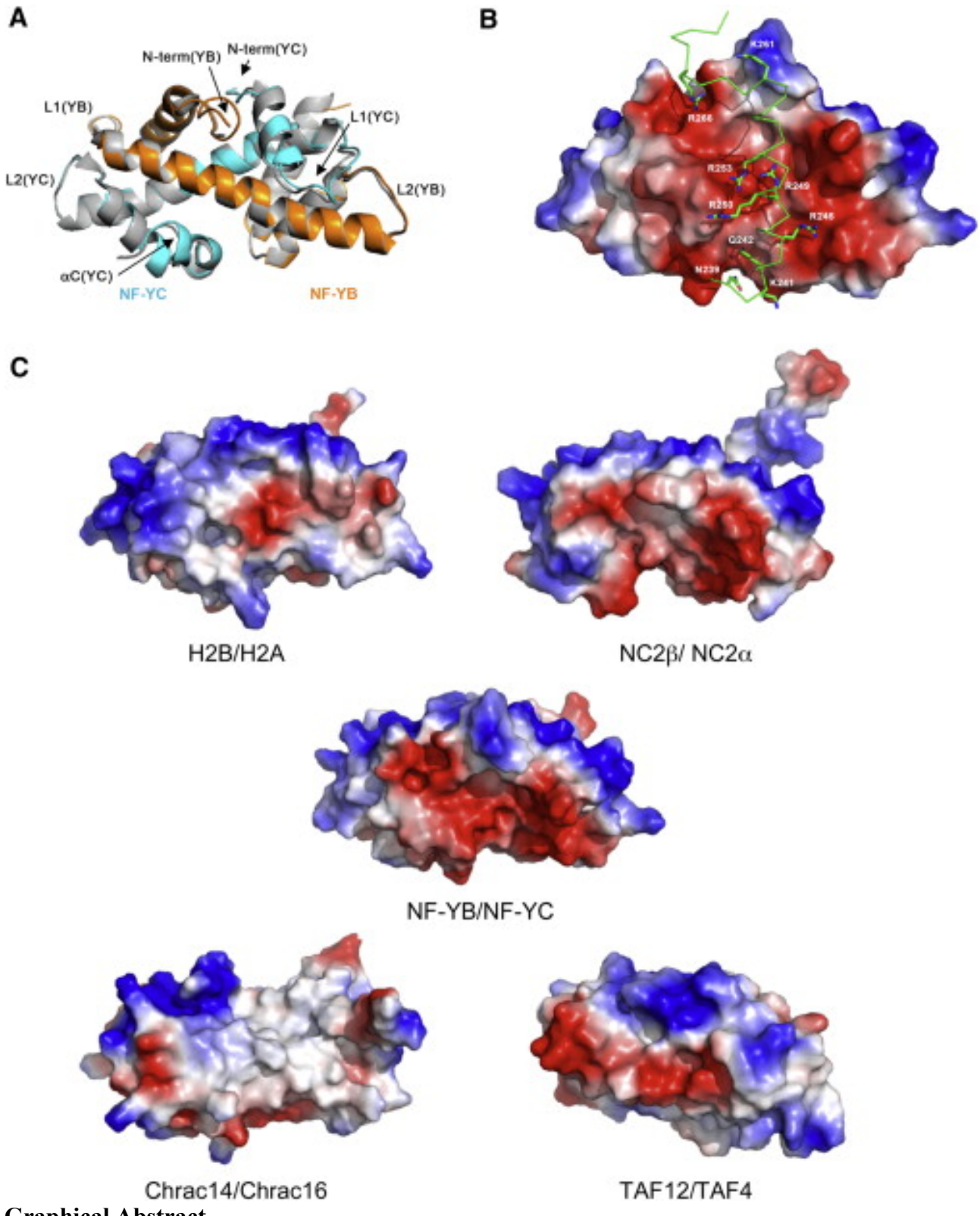

Graphical Abstract

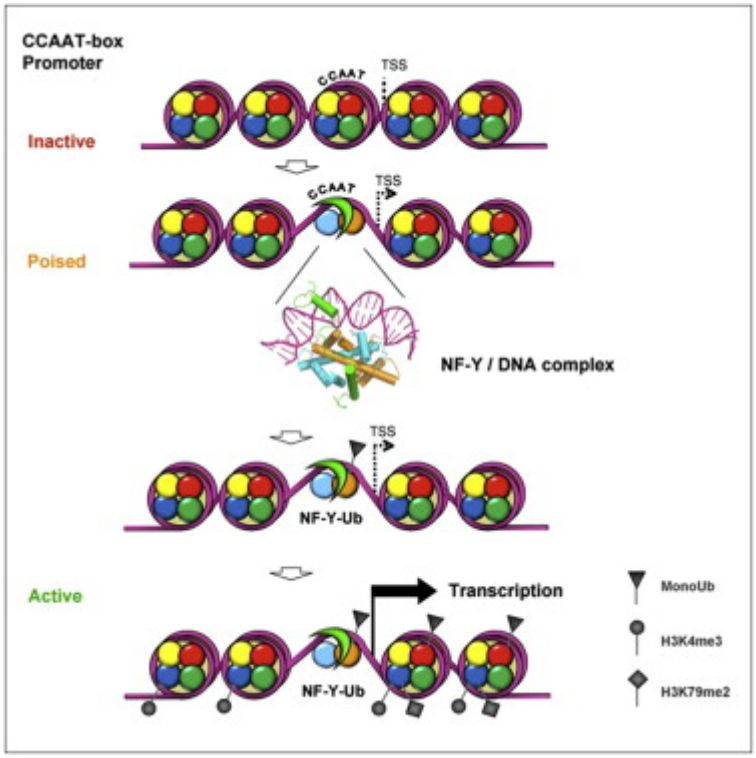

Figure options

Highlights

► 3D structure of NF-Y/CCAAT shows close relationships to core histones H2A/H2B ► NF-YA displays a sequence-specific DNA minor groove-binding module ► Histone H2B and NF-YB share a functional posttranslational modification ► NF-Y binding and monoubiquitination are early events in gene activation

---

Introduction

Initiation of transcription is regulated by sequence-specific binding of transcription factors (TFs) that recognize DNA elements in promoters and enhancers, and interface with chromatin structures. NF-Y, also termed CBF, is a trimeric protein composed of NF-YA, NF-YB, and NF-YC subunits, all of which are necessary for binding to the CCAAT box, which occurs in 30% of eukaryotic promoters (Dolfini et al., 2009). The CCAAT box location within promoters is fixed at −60/−100 nucleotides from the transcriptional start site (TSS) and, whenever tested, has been shown to be crucial for promoter activity. The three subunits are evolutionarily strongly conserved in all eukaryotes, and to form the NF-Y/CCAAT complex, the NF-YA subunit must first associate with NF-YB/NF-YC, which are in turn known to heterodimerize via their histone-fold domains (HFDs) (Romier et al., 2003); HFDs host at least three helices (α1, α2, and α3), separated by two loops (L1 and L2). In addition to core histones, the same secondary structure arrangement is found in several nuclear proteins involved in various aspects of DNA metabolism; these include (1) most of the TATA-binding protein (TBP)-associated factors (TAFs), components of TFIID (Gangloff et al., 2001), of SAGA, and ATAC coactivator complexes (Nagy and Tora, 2007); (2) the TBP/TATA-binding negative cofactor 2 (NC2α/β) (Kamada et al., 2001); and (3) the small subunits of the nucleosome-remodeling complex CHRAC (Corona et al., 2000; Poot et al., 2000), one of which (Dpb4) also dimerizes with Dpb3 as part of DNA polymerase ε (Li et al., 2000). Despite 15%–18%

sequence identity within the 65–80 amino acid HFD, structural studies of TAFs, NC2α/β, NF-YB/NF-YC, and Chrac14/Chrac16 reported closely related tertiary structures (Gangloff et al., 2001; Werten et al., 2002; Kamada et al., 2001; Romier et al., 2003; Hartlepp et al., 2005). Additionally, plant-specific homologs of NF-YA have also been characterized, notably TFs of the CCT family (CONSTANS [CO], CONSTANS-LIKE, TOC1), involved in regulation of flowering time (Wenkel et al., 2006). From the functional viewpoint, NF-Y is considered as a facilitator of TF binding and an architectural promoter organizer; the molecular details underlying its role are, however, largely unknown.

NF-Y binding to DNA is also important for the establishment of histone posttranslational modifications (PTMs) such as H3K4me3, H3K79me2, and H3K36me3, as well as some acetylations, on active promoters, through recruitment of relevant enzymes (reviewed in Dolfini et al., 2012). Specific histone PTMs are marks of a peculiar chromatin environment, some are associated with accessible-active chromatin, others with heterochromatin, either constitutive or facultative (Suganuma and Workman, 2011). For instance, monoubiquitination of H2B at Lys120 (Lys123 in yeast) is an early event in the establishment of a chromatin environment conducive to transcription (Robzyk et al., 2000; reviewed by Laribee et al., 2007; Weake and Workman, 2008); H3K4me3 and H3K79me2 modifications follow in regions that are transcribed, or poised to rapid induction (Ruthenburg et al., 2007). Their occurrence in vivo has been confirmed by several genome-wide studies (Ernst et al., 2011).

What determines the location of epigenetic marks on genomes is a question of wide general relevance. Because binding of TFs and cofactors is a hallmark of expression by signaling the location of promoters to the Pol II machinery, it may be postulated that histone marks on promoters are determined by the previous binding of sequence-specific TFs, such as NF-Y. We report here the crystal structure of the binary complex composed of the NF-Y trimer and a CCAAT box containing DNA fragment (25 bp); our results detail the structural basis of a sequence-specific, histone-like, mode of DNA binding. Starting from structural considerations, we detail the functional behavior of a NF-YB PTM at Lys138, highly reminiscent of Lys120 monoubiquitination of histone H2B.

Results

Overall Architecture of the NF-Y/DNA Complex

The crystal structure of the evolutionarily conserved domains of the NF-Y heterotrimer in complex with a 25 bp oligonucleotide containing the HSP70 promoter CCAAT sequence (Figure S1A available online) (Li et al., 1998) is reported here at 3.1 Å resolution (Figures 1, 2B, and S2; Table S1). The head-to-tail assembly of NF-YB and NF-YC subunits provides a stable-compact dimeric scaffold, ready for association of NF-YA and DNA binding. The HFD subunits within the NF-Y trimer match closely the isolated NF-YB/NF-YC dimeric structure reported earlier (Romier et al., 2003) (rmsd of 0.73 Å over 164 Cα pairs), with some notable differences (Figure 2A): (1) NF-YB and NF-YC N termini are structurally better defined in the DNA complex; (2) the bidentate salt bridge between Arg108(YB) and Asp115(YB) (residues are labeled with their respective NF-YA, -YB, and -YC subunit identifiers), reported for the isolated dimer, is absent in the NF-Y/DNA structure, where poor density is present for the Arg108(YB) side chain, and the Asp115(YB) side chain is partly differently oriented; and (3) the NF-YC L1 region and the αC helix are slightly shifted, likely because of their interaction with DNA and NF-YA, respectively. Notably, the NF-YC αC helix contributes, together with NF-YC α1 and NF-YB α2, to the formation of a wide and negatively charged surface groove responsible for binding of the NF-YA N-terminal helix (Figures 1B and 2B).

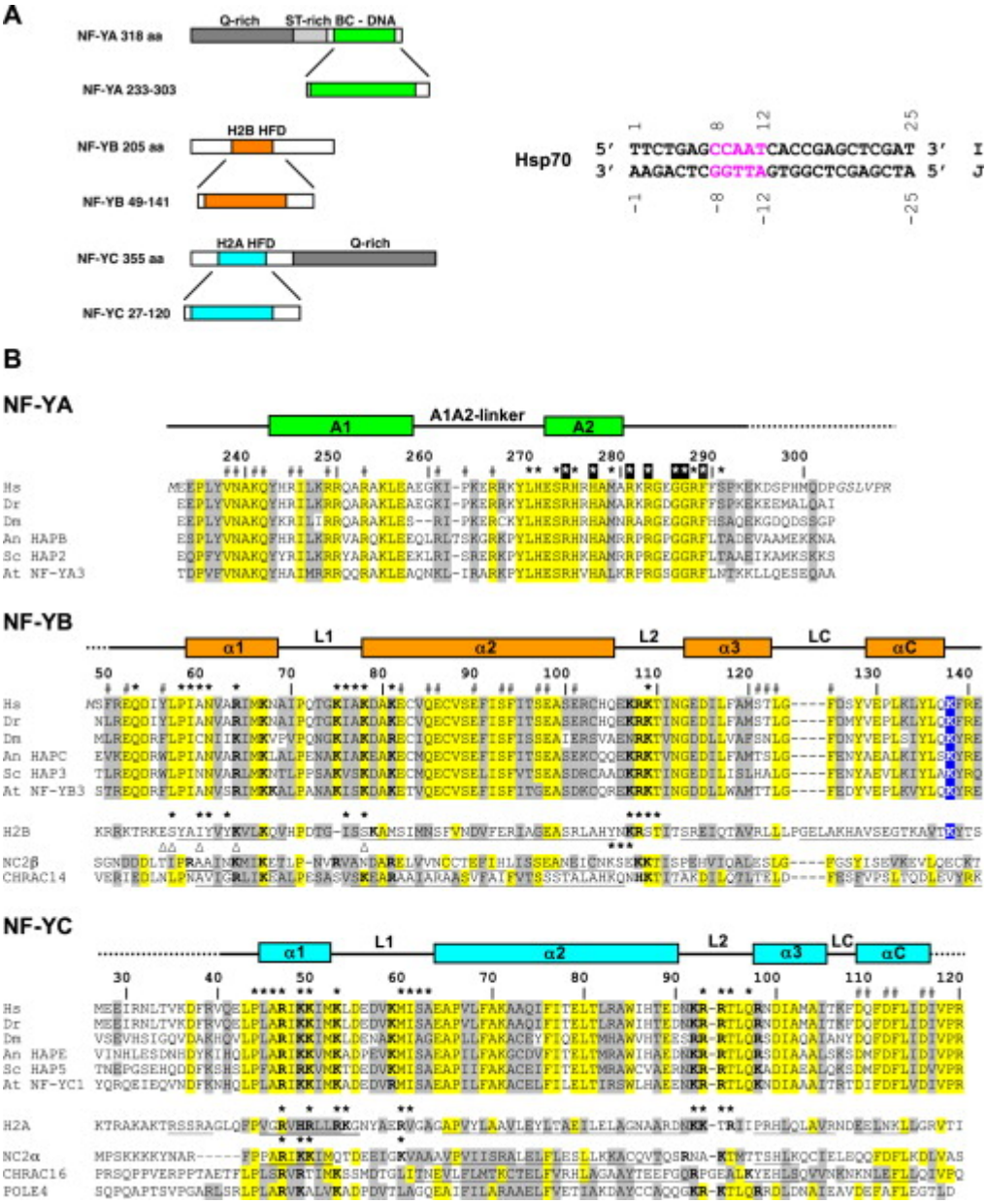

Figure S1.

NF-Y Subunits and Sequence Alignments, Related to Figure 1

(A) Schematic representation of the NF-Y full length protein subunits, and location of the constructs used for crystallization of the trimer, with sequence of the 25 bp DNA oligonucleotide. (Left) Color-shaded boxes highlight the evolutionarily conserved NF-YB/NF-YC/DNA binding domain (BC-DNA; green) in NF-YA, and H2B-like or H2A-like HFD domains in NF-YB and NF-YC (orange and cyan, respectively). Shaded gray boxes indicate the locations of Gln-rich domains in NF-YA and NF-YC (Q-Rich), and Ser/Thr rich domain of NF-YA (ST-rich; light gray). (Right) Sequence of the 25 bp DNA oligonucleotide used in this work for the NF-Y/DNA complex crystallization, derived from the NF-Y target Hsp70 promoter (Li et al., 1998), corresponding to nt −59 to −83 of the human HSPA1A gene promoter sequence (TRED acc.no. 35259), with numbering of bases as labeled in the structure on the corresponding I and J strands.

(B) Sequence alignments of the core regions of NF-YA (233-303), NF-YB (49-141), and NF-YC (27-120) from human (Hs), zebrafish (Dr), *Drosophila melanogaster* (Dm),

Aspergillus nidulans (An HAPB, An HAPC and An HAPE), *Saccharomyces cerevisiae* (Sc HAP2, Sc HAP3 and Sc HAP5), and one of the *Arabidopsis thaliana* homologs for each NF-Y subunit (At NF-YA3, At NF-YB3 and At NF-YC1). Throughout the paper the mouse NF-YA, mouse NF-YB, and human NF-YC numbering is used for the respective subunits. Identical residues in all NF-Y sequences and highly conserved residues (>80% sequence conservation) are highlighted by yellow and gray shadings, respectively. Blue shading highlights H2B Lys120, Lys138 in NF-YB, and corresponding conserved residues. Secondary structure elements (bars for helices and solid lines for coils), as observed in the NF-Y structure, are shown on the top of the sequence alignment. Dotted lines indicate regions present in the crystals that are not seen in the electron density; in *Italics*, foreign sequences present in the NF-Y recombinant proteins that were added for purification purposes. The NF-YB and NF-YC sequences have been structurally aligned also with *Xenopus laevis* H2B and H2A (PDB entry 1AOI), human NC2β and NC2α (PDB entry 1JF1), *Drosophila melanogaster* Chrac14 and Chrac16 (PDB entry 2BYM) (homologs to human POLE3 and Chrac15, respectively) (Kukimoto et al., 2004; Corona et al., 2000). For NF-YC the sequence of human H2A-like POLE4 is also aligned (Li et al., 2000). Residues belonging to HFD helices in H2A/H2B, NC2α/NC2β, and Chrac14/Chrac16 are underlined (Luger et al., 1997; Kamada et al., 2001; Hartlepp et al., 2005). Residues identical and similar to human NF-Y are highlighted by yellow and gray boxes, respectively. The hash (#) symbol is associated to residues involved in NF-Y trimerization. Asterisks indicate residues involved in DNA interactions. Boxed asterisks indicate residues involved in DNA-base interactions. DNA interacting residues of H2A/H2B and NC2α/NC2β are highlighted similarly; the Δ symbol indicates NC2β residues interacting with a symmetry related oligonucleotide in the crystal packing (Luger and Richmond, 1998; Kamada et al., 2001). Basic residues at the DNA-interacting regions (α1, L1, and L2) are highlighted in bold.

Figure options

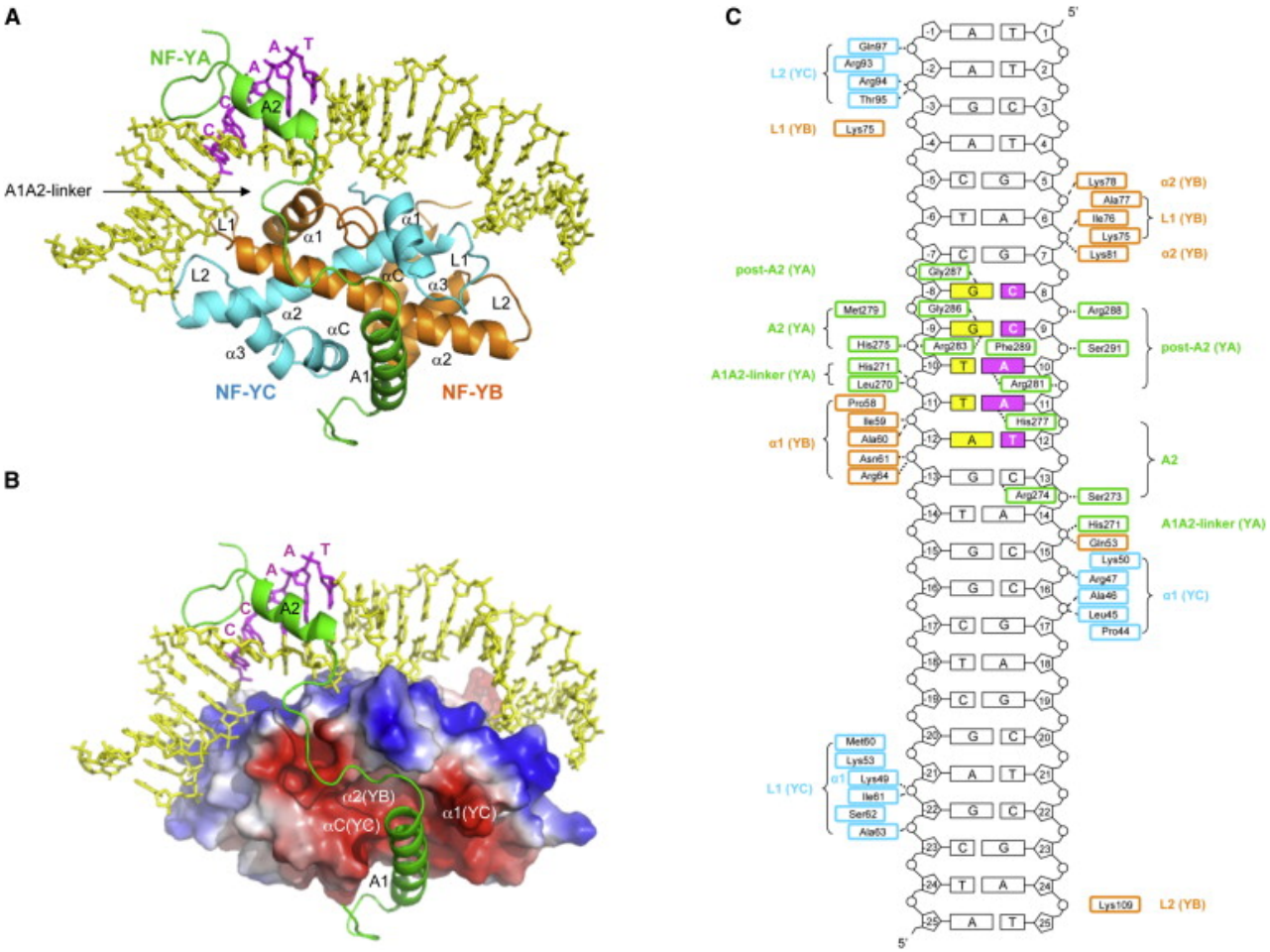

Figure 1.

Overall Structure of the NF-Y/DNA Complex and Schematic Representation of DNA Contacts

(A) Ribbon representations of the NF-YA/-YB/-YC heterotrimer in complex with the HSP70 25 bp CCAAT box oligonucleotide; the key secondary structure elements are labeled. NF-YA, NF-YB, and NF-YC are colored in green, orange, and cyan, respectively, and the DNA molecule in yellow, with CCAAT nucleotides highlighted in magenta.

(B) Electrostatic surface of the NF-YB/NF-YC dimer. Blue and red colors indicate positively and negatively charged regions, respectively. NF-YA and DNA are represented in ribbon and stick models color coded as above.

(C) DNA contacts made by NF-Y are indicated as follows, with subunit color coding as in (A): dotted lines indicate hydrogen bonds and salt bridges provided by amino acid side chains; dashed lines indicate hydrogen bonds involving protein main-chain atoms; residues boxed, but devoid of dashed/dotted lines, provide NF-Y/DNA van der Waals contacts.

See also Table S1 and Figure S1.

Figure options

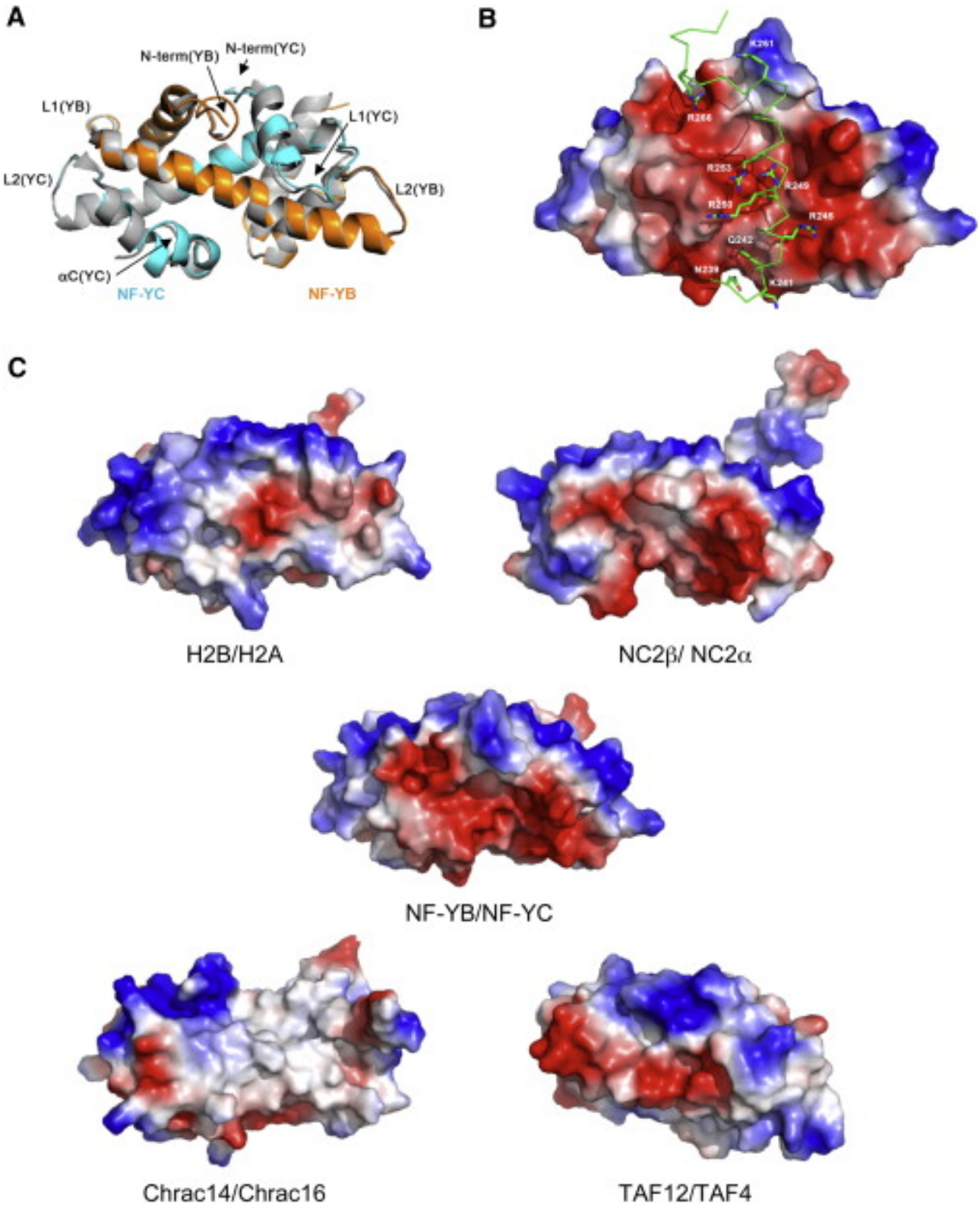

Figure 2.

NF-Y HFD Subunits in the NF-Y/DNA Complex and in the Free Dimer Structure, Interactions with NF-YA, and Comparison to Other HFD Proteins

(A) Ribbon representation of the superimposition of NF-YB/NF-YC HFD dimer in the CCAAT box complex (color codes as in Figure 1) and in the isolated dimeric form (gray color) (PDB 1N1J). Arrows point to the most structurally divergent regions.

(B) Matching of the A1 helix polar residues with the NF-YB/NF-YC interface. The relevant NF-YA region is shown as ribbon (main chain) and sticks (side chains). For clarity, one-letter codes are used for residue identification.

(C) Electrostatic surface of HFD core dimers (PDB codes for H2B/H2A [without histone tails], NC2β/α, Chrac14/Chrac16, and TAF12/TAF4 are 1AOI, 1JFI, 2BYK, and 1H3O, respectively) brought to a common orientation after superimposition on the NF-YB/NF-YC dimer (PDB 4AWL; in the orientation of Figure 1). The positively charged DNA-interacting surface (blue color) falls on the top of each protein molecule.

See also Table S2 and Figure S2.

Figure options

Figure S2.

Electron Density at the NF-Y-DNA Interface, Related to Figure 2

(A and B) Stereo view of a representative 3.1 Å resolution omit map contoured at 1.0σ, showing (A) the NF-YA region (magenta mesh) and the interfacing DNA CCAAT box region (green mesh) and (B) the DNA-base intercalation of Phe289(YA). Selected residues and bases are indicated.

Figure options

The NF-YA subunit displays an elongated structure that hosts the N-terminal A1 (residues 243–258) and the C-terminal A2 helices (272–280), followed by a loop containing a GxGGRF motif (x = any residue; 284–289); the two helices are separated by a 15-residue linker loop (A1A2 linker) (Figures 1A, 1B, and S1B). Most of NF-YA-exposed residues are polar and/or positively charged (Figure 2B). The NF-YA A1 helix contacts extensively the HFD dimer (contact interface of 1,760 $Å^2$). The most relevant interactions stabilizing the NF-Y heterotrimer are Asn239(YA) with Asp109(YC) and with Asp112(YC); Gln242(YA) with the backbone atoms of Leu123(YB) and Phe113(YC); Arg245(YA) with Glu98(YB) and Glu101(YB); Arg249(YA) with Glu90(YB); Arg250(YA) with Asp116(YC); and a cluster of hydrophobic residues hosting Ile246(YA), Phe94(YB), and Ile115(YB) (Table S2; Figure 2B). Most of these residues were proven crucial for NF-Y heterotrimerization in previous mutational studies (Table S3). The A1A2 linker segment also contributes to heterotrimerization, Lys261(YA), Pro263(YA), Arg267(YA) (main-chain atoms), and Arg266(YA) (side chain) being involved in intramolecular contacts (Table S2; Figure 2B). Structurally, the A1A2 linker adopts an extended conformation that can provide the conformational flexibility required to direct the NF-YA chain toward DNA, at the same time optimizing electrostatic interactions at the NF-YA/NF-YB/NF-YC interface.

NF-Y Binds and Distorts DNA at the Minor Groove

NF-Y/DNA complex stabilization involves at least 41 residues (Figure 1C), in keeping with its stunning stability (K_D values in the 10^{-10}–10^{-11} M range; Dolfini et al., 2012). Protein-DNA contacts are distributed along the whole length of the 25 bp oligonucleotide; two main protein-DNA-binding regions can, however, be roughly distinguished as provided by the NF-YA chain and by the HFD dimer, respectively, discussed in the following two sections.

A key structural feature of the NF-Y/DNA complex is the insertion of NF-YA A2 helix into the DNA minor groove, resulting in a strong positive roll of 48° at the center of the CCAAT box (base pairs 9 and 10), mainly responsible for a global DNA bending of about 80° (Figures 1A, 1B, 3A, and 3B). Overall, the bound DNA achieves a relatively standard B conformation (average helical twist of 36.1°), maintaining a constant major groove width along the 25 bp stretch (average of 16.4 Å). In contrast, the minor groove is strikingly widened at the CCAAT box, with a maximum of 19.1 Å at the first adenine of the CCAAT box. Such DNA distortion is entirely consistent with previous circular permutation experiments performed on several sites, including the HSP70 CCAAT, which showed bending with angles centered precisely on the CCAAT box, curvatures varying marginally according to the CCAAT-flanking sequences, and markedly depending on the NF-Y constructs: specifically, with NF-Y constructs similar to the one used here, bending angles of 78°–80° were observed by Liberati et al. (1999). Furthermore, the DNA phosphates contacted by NF-Y in our structure (Figure 1C) match the interaction sites previously mapped by hydroxyl radical footprinting (Bi et al., 1997).

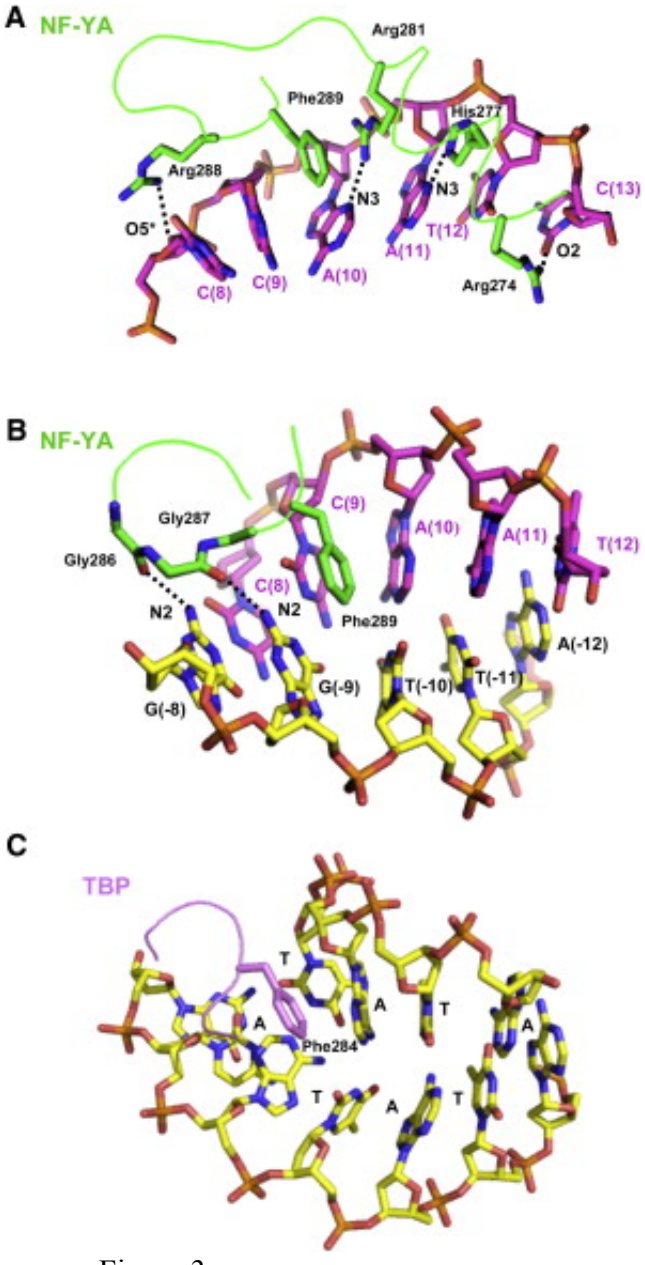

Figure 3.

Specific Interactions in NF-Y/CCAAT Recognition

(A) Interactions of NF-YA and the CCAAT DNA strand (magenta) are indicated. The complementary DNA strand has been omitted for clarity. Key residues/atoms are labeled, and selected hydrogen bonds are shown by dotted lines.

(B) Positive roll of 48° between base pairs 9 and 10 due to the insertion of NF-YA Phe289 side chain. Interactions of NF-YA (green color) and the CCAAT complementary DNA strand (yellow) are highlighted.

(C) TBP minor groove interactions with DNA. Phe284, which inserts into the first base pair of the targeted sequence, is shown (PDB 1TGH; Juo et al., 1996).

See also Table S3 and Figure S3.

Figure options

CCAAT Box Recognition by NF-YA

Base recognition within the CCAAT box relies on the NF-YA A2 helix and the following GxGGRF motif, both deeply located into the CCAAT minor groove region (Figures 1, 3A, and 3B). NF-Y/CCAAT-box-specific interactions link residues Arg274(YA) to O2 atom of C(13), His277(YA) to N3 atom of A(11), Arg281(YA) to N3 atom of A(10) (Figure 3A), and Arg283(YA) to N3 atom of G(−9) (Figure 1C). The presence of His and Arg residues interacting with the N3 atoms of A(10) and A(11) in the CCAAT box contributes to specificity by restricting the presence of G bases for steric reasons. Accordingly, mutants of these residues abolish DNA binding (Table S3).

The GxGGRF motif displays a kinked backbone (where Gly286(YA) and Gly287(YA) adopt a left-handed helical conformation) that allows minor groove insertion of Phe289(YA) between the C(9)—G(−9) and the A(10)—T(−10) consecutive base pairs, and close proximity of Gly286(YA) and Gly287(YA) carbonyl O atoms to the bases of the CCAAT complementary DNA strand (Figures 3B and 1C). Such a set of interactions is crucial for specificity because it restricts the interaction with the G exocyclic N2 amino group of G—C base pairs in the CCAAT box. The observed structure explains also why the G→I (inosine) substitution at position −8 or −9 severely impairs DNA binding (Ronchi et al., 1995). Not surprisingly, the GxGGR loop and Phe289(YA) are conserved (Figure S1B), and their mutations abolish DNA binding (Table S3). Remarkably, the insertion of Phe289(YA) into the minor groove is reminiscent of TBP minor groove interactions with DNA, where residues Phe284 and Phe193 insert into the first and last base pairs of the TATA sequence, respectively, twice kinking the DNA (Figure 3C) (Kim et al., 1993; Juo et al., 1996; Kamada et al., 2001). Furthermore, Arg288(YA) interacts with the C(9) phosphate, together with seven additional NF-YA-conserved residues that provide interactions to the DNA phosphate backbone (Figures 3A and 1C).

In plants, the sequence similarity between NF-YA and its CCT homolog CO, striking at the A2 helix, is relaxed at Gly284(YA) and Gly286(YA) of the GxGGRF motif (Figure S3): thus, the loop and the consequent DNA-reading capacity may vary, suggesting that CO might have evolved to recognize slight variations of CCAAT, with a different 5′ end. On the other hand, the N-terminal region of the CCT domain of CO is rich in basic residues as the NF-YA A1 region, possibly being suited for heterotrimeric assembly with NF-YB/NF-YC.

Figure S3.

Sequence Alignment of the CCT Domains, Related to Figure 3

CCT domains of human (Hs) NF-YA, *A. thaliana* (At) NF-YA3 and NF-YA10, CONSTANS (CO), CONSTANS-Like 9 (COL9), and TIMING OF CAB1 (TOC1). Color shading of residues as in Figure S1, with residues identical and similar to human NF-Y highlighted in yellow and gray, respectively. The hash (#) symbol is associated to residues involved in NF-Y trimerization. Asterisks indicate residues involved in DNA interactions. Black shaded asterisks indicate residues involved in DNA-base interactions. Dots (•) indicate the position of CCT domain mutations identified in plants (Wenkel et al., 2006). The GxGGRF (CCAAT binding) motif of Hs NF-YA and the corresponding sequences in the other CCT domains are boxed.

Figure options

NF-YB/NF-YC Display Structural and DNA-Binding Properties Similar to H2A/H2B and NC2α/β

The overall stability of the NF-Y/DNA complex is coded by favorable van der Waals and electrostatic interactions established between the highly basic upper surface of the NF-YB/NF-YC dimer and the negatively charged DNA sugar-phosphate backbone (Figures 1B and 2C); such interactions appear devoid of DNA sequence specificity. In fact, the majority of such polar interactions involve protein backbone atoms, whereas only the side chains of Gln53(YB), Asn61(YB), Arg64(YB), Lys81(YB), Arg47(YC), Lys49(YC), and Gln97(YC) contact directly the DNA phosphates (Figure 1C). Several additional van der Waals contacts are also present: the α1-α1 region (Figures S4A and S4B) and the two L1-L2 loops (Figures S4C–S4F) build the central part and the two sides of the DNA-backbone contact region, respectively. These interactions are in full agreement with extensive mutagenesis data (Table S3), and with engineering experiments that swapped the α1 helices of NF-YB and NF-YC with other HFD-based proteins indicating that integrity of α1 is essential for DNA binding, and that residues Arg47(YC), Lys49(YC), and Asn61(YB) are crucial (Zemzoumi et al., 1999) (Figures 1C, S4A, S4B, and S4D).

Figure S4.

Details of the NF-Y HFD-DNA Interactions, Related to Figure 4

(A–F) NF-Y HFD/DNA interactions at the α1, L1, and L2 structural elements, for NF-YB (A, C, and E, respectively), and NF-YC (B, D, and F, respectively). Subunit color coding as in Figure 1. Dotted lines indicate protein-DNA hydrogen bonds and salt bridges.

Figure options

The structure and the DNA-binding mode of the NF-YB/NF-YC dimer are highly reminiscent of that of other HFDs (Figure 2C). Comparison of NF-YB/NF-YC dimer with histones H2B/H2A (Figure 4A) revealed a rmsd of 1.5 Å between 125 Cα pairs. Despite such relatively low rmsd value, some structural differences are worth noticing. NF-YB diverges from H2B at the N terminus, where H2B hosts the histone tail; at the L1 region, where NF-YB is shifted due to the widening of the DNA minor groove at the CCAAT box, and to a one amino acid insertion relative to H2B (Figure S1B); and at the LC region (between helix α3 and αC), where NF-YB contacts NF-YA

(Table S2) and H2B hosts a four-residue insertion (Figure S1B). NF-YC differs from H2A in the α1-L1 region, where H2A interfaces to the H2B N terminus and to the L2 loop of the H2A′ subunit within the nucleosome; and in the LC-αC region, where NF-YC contacts NF-YA (Figure 1B; Table S2). Structural differences between the H2B/H2A and NF-YB/NF-YC dimers at the regions where the NF-Y HFD module contacts NF-YA are coupled to poor conservation in H2B/H2A of negatively charged residues important for NF-Y trimerization (Figures 2C and S1B). Despite this, it is remarkable that NF-YC/NF-YB and H2A/H2B display strongly similar overall DNA-binding modes (Figure 4A), with conservation of the α1-α1 and the L1-L2 contacts to DNA (Figures S1B and S4). The histone-fold heterodimer of Chrac14/Chrac16 (Hartlepp et al., 2005) resembles the geometry of NF-YB/NF-YC (Figure 2C), but it lacks several side-chain interactions to DNA (Figure S1B). The positive-charge distribution on the TAF12/TAF4 subunits of TFIID is partial, although they support DNA binding to subclasses of core promoters (Wright et al., 2006; Gazit et al., 2009).

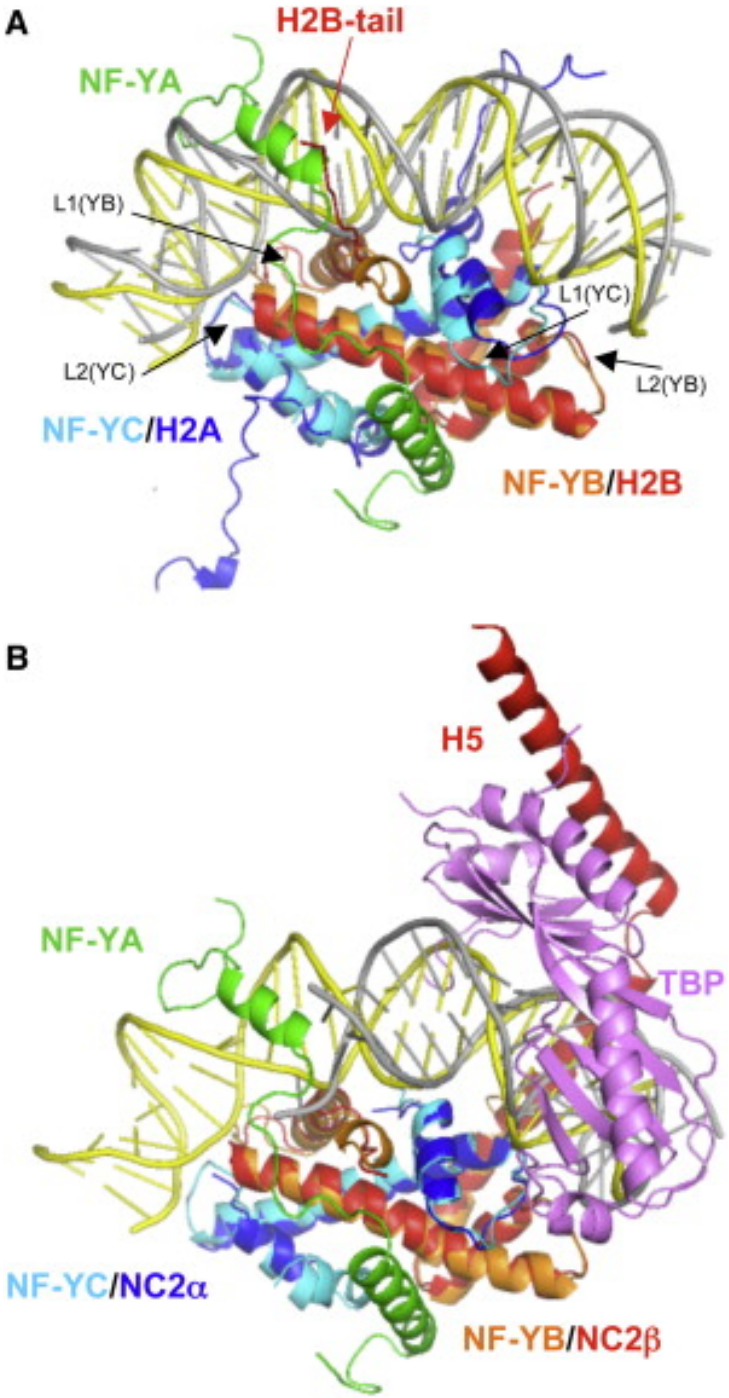

Figure 4.

DNA-Binding Mode of NF-Y Compared to Other HFD Proteins

(A) NF-Y subunits and the 25-bp-bound DNA (color coded as in Figure 1) are shown after superimposition of the NF-YB/NF-YC dimer on the nucleosome H2A/H2B histone pair (blue and red, respectively). The histone proteins and the 25-bp-bound DNA (in gray) are those of *X. laevis* nucleosome (PDB 1AOI; Luger et al., 1997). The H2B N-terminal tail location is indicated by a red arrow.

(B) Overlay of the NF-YB/NF-YC dimer to the NC2α/β HFD subunits, in blue and red, respectively (PDB 1JF1; Kamada et al., 2001). The associated TBP is shown in magenta.

NC2β helix H5 at the TBP interface is highlighted; NC2α/β-associated DNA fragment is shown in gray.

See also Figure S4.

Figure options

The shorter length of our crystallization oligonucleotide (25 bp) relative to the 36–37 bp required to span a heterodimer within the nucleosome (Luger et al., 1997) partly limits the NF-YB-DNA interactions at the L2 sites, which can therefore be expected to be more extended, likely involving Lys107(YB) (Figures 1C and S4E). Thus, the DNA distortion due to the insertion of NF-YA A2 helix in the CCAAT box region is compensated by local protein readjustments that allow maintaining a canonical nucleosome-like DNA-binding structure. Strikingly, the overlay of the whole NF-Y structure on the H2A/H2B dimer positions NF-YA helix A2 at a site matching the location of the H2B histone tail that exits the nucleosome at the DNA minor groove (Figure 4A), suggesting an evolutionary mechanism whereby the NF-YB/NF-YC dimer would have recruited a non-HFD protein subunit (NF-YA) to mimic the H2B histone tail, thus achieving DNA recognition specificity.

The NF-Y dimeric structure and DNA-binding mode are also similar to those of NC2α/β, in complex with TBP-DNA (Figure 4B): the HFD dimers superimpose with a rmsd of 1.1 Å (over 140 Cα pairs), the main structural deviations being located at the N terminus of NF-YB (residues 50–55) due to the interactions with NF-YA (Table S2), and in the L1 region (residues 71–77), due to the interactions with DNA (Figure S4C). On the NF-YC side, differences are localized at the first three N-terminal residues, and at the L2 loop (residues 91–94), which is disordered in NC2α (Kamada et al., 2001). Similarly, the C-terminal region of NC2α is disordered, whereas in NF-YC, a well-defined αC helix contributes to NF-Y trimerization via interactions with NF-YA (Figure 4B). Overall, despite limited insight available for the NC2α/β DNA interactions, due to the short length of the bound DNA (Kamada et al., 2001), DNA contacts involving NC2α at α1, L1, and L2, and NC2β at L2, are essentially equivalent in NF-YC and NF-YB, respectively (Figure S1B), and sequence variations in the NC2 HFD prevent NF-YA binding, as previously assessed and discussed (Zemzoumi et al., 1999, Romier et al., 2003).

NF-YB Is Monoubiquitinated at Lys138 in the HFD αC

The structural results prompted us to investigate functional similarities linking NF-YB and H2B: inspection of the NF-Y/DNA structure shows that Lys138(YB) and H2B Lys120 are similarly located and accessible when the nucleosome particle and NF-Y/CCAAT are overlayed (Figure 5A). Because monoubiquitination of H2B Lys120 plays a key role in transcription, we hypothesized that NF-YB might also be monoubiquitinated in vivo. Endogenous NF-Y was immunoprecipitated with an anti-NF-YB antibody, and western blot (WB) analysis was performed with an anti-ubiquitin (Ub) antibody. In the NF-YB-immunoprecipitated material, we detected a 40 kDa band, not present in the control immunoprecipitate (IP) (Figure 5B), whose molecular weight (MW) is consistent with the addition of a mono-Ub moiety to the NF-YB 32 kDa subunit. Two additional bands around 50 kDa were also observed, whose nature was not further analyzed. To verify NF-YB ubiquitination, we cotransfected Cos-1 cells with Flag-NF-YB and/or HA-tagged Ub (HA-Ub) expression vectors: analysis of total extracts with an anti-NF-YB antibody detected bands with MWs corresponding to endogenous NF-YB and Flag-NF-YB in transfected cells, and a band consistent with monoubiquitinated Flag-NF-YB when HA-Ub was cotransfected with Flag-NF-YB (Figure 5C, top). Immunoprecipitation of transfected cell extracts with anti-NF-YB was performed, followed by WB: the anti-HA blot revealed the presence of a 50 kDa HA-Ubiquitinated protein

when Flag-NF-YB and HA-Ub were transfected together, consistent with the MW increase of Flag-NF-YB (Figure 5C, bottom). When blots were probed with anti-Flag antibodies, the slower mobility (HA positive) pattern of NF-YB was confirmed (Figure 5C, bottom). These data indicate that NF-YB is monoubiquitinated in vivo.

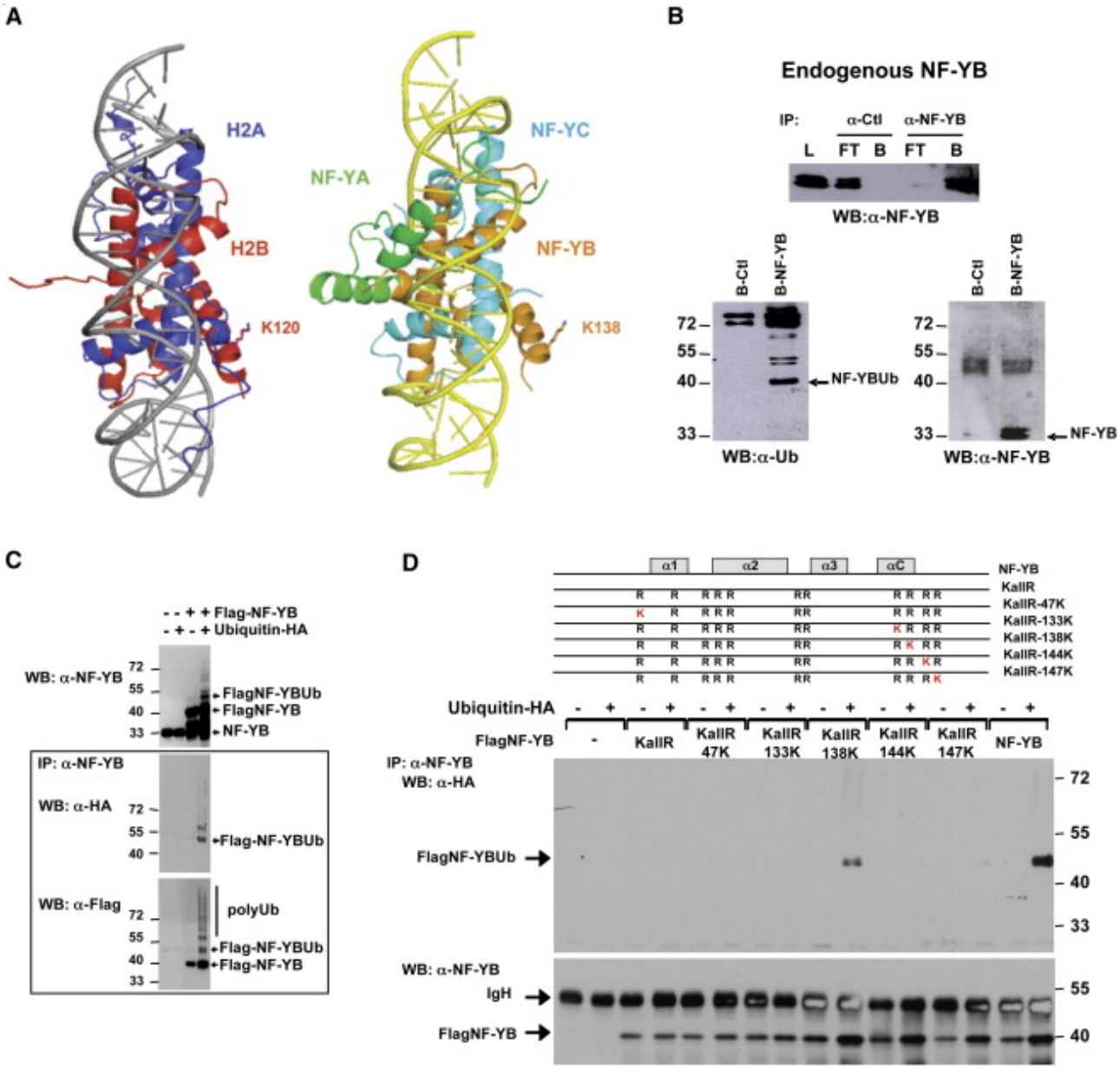

Figure 5.

NF-YB Is Monoubiquitinated In Vivo on Lys 138

(A) The H2A/H2B histone pair (blue and red, respectively) with 25 bp DNA (gray color) of the *X. laevis* nucleosome (left) is compared with the NF-Y complex with the 25 bp HSP70 CCAAT box DNA (yellow color) (right). The two complexes have been brought to the same orientation by superimposing NF-YB/NF-YC (orange and cyan colors, respectively) to H2B/H2A. The location of residue Lys138(YB), equivalent to H2B Lys120, is highlighted.

(B) Immunoprecipitation with anti-NF-YB and control (Ctl) (anti-thioredoxin) antibodies was performed with NIH 3T3 nuclear extracts. (Top) The WB with the anti-NF-YB antibody (L, input; FT, flowthrough; B, bound). The bound material was assayed in WB

with an anti-Ub antibody that recognizes mono- and polyubiquitinated proteins (lower-left) and anti-NF-YB (lower-right).

(C) Overexpression of HA-Ub and Flag-NF-YB was performed in Cos-1 cells. Extracts of transfected cells were analyzed in WBs with anti-NF-YB (top) and after immunoprecipitation with the anti-HA and anti-Flag (bottom) antibodies. The resulting NF-YB bands are indicated.

(D) Overexpression of Flag-NF-YB, WT and mutants, with HA-Ub, as in (C). Immunoprecipitations with anti-NF-YB of transfected cell extracts were analyzed in WB with anti-HA (top) and anti-NF-YB (bottom). The NF-YB bands are indicated on the left. The immunoglobulin heavy chain (IgH) is also indicated. Note the shading of the Flag-NF-YB-Ub band by the IgH.

Figure options

To pinpoint the residue(s) involved, the 11 Lys residues of Flag-tagged NF-YB were mutated to Arg, obtaining the NF-YB-K-all-R vector: thereafter, single Arg residues were mutated back to Lys, focusing on Lys133(YB) and Lys138(YB), fully exposed to the solvent in our NF-Y/DNA complex, while excluding residues in contact with DNA (Lys75(YB), Lys78(YB), Lys81(YB), Lys107(YB), and Lys109(YB)), or buried at the NF-YB/DNA interface (Lys67(YB)). Additionally, we checked single-site back-mutated proteins at Lys47(YB), Lys144(YB), and Lys147(YB) (Figure 5D), not present in the crystallized NF-YB construct (Figure S1B). These mutants were transiently transfected with and without the HA-Ub vector: none of the Flag-YB mutants was positive without HA-Ub, and only Arg138(YB)→Lys showed the 50 kDa band when cotransfected with HA-Ub (Figure 5D, top, WB: α-HA). All mutants were equally expressed (Figure 5D, bottom, WB: α-NF-YB). We conclude that Lys138(YB) is a monoubiquitination site structurally equivalent to histone H2B Lys120. This result is in agreement with a recent report on large-scale proteomic analysis of ubiquitinated proteins by Wagner et al. (2011).

NF-YB Ubiquitination Is Required for H2B Ubiquitination and H3-Positive Methylations

Impairment of NF-Y binding to CCAAT promoters causes a significant drop in the levels of histone H3 methylations (Dolfini et al., 2012), raising the question of whether NF-Y binding plays a role for H2BK120-Ub. We employed the NF-YA dominant-negative YAm29 mutant (YA-DN), harboring a mutation in the A2 helix, which results in association with endogenous NF-YB/NF-YC and removal of the NF-Y trimer from CCAAT boxes, coupled to MNase-chromatin immunoprecipitation (ChIP) of synchronized G2/M-arrested HCT116 cells (Gatta and Mantovani, 2010). ChIP assays on the active CyclinB2 with anti-NF-YB and H2BK120-Ub antibodies show that NF-Y was efficiently removed by YA-DN and that the levels of H2BK120-Ub dropped dramatically in the +1, +2, and +3 nucleosomes (Figure S5A, left). The same was observed on another G2/M promoter, CDC2, and on the housekeeping SON (Figure S5A, right). Note the increase in H2B on promoters upon NF-Y removal. Inactive G1/S-specific or tissue-specific promoters, negative for NF-Y binding, showed no effect of the YA-DN. We also used shRNA targeting NF-YB, observing essentially the same drop in H2BK120-Ub (Figure S5B). We conclude that promoter binding of NF-Y is necessary for H2BK120-Ub deposition in transcribed regions.

Figure S5.

NF-Y Binding Is Required for H2B Monoubiquitination, Related to Figure 6

(A) Analysis of the distribution of NF-YB subunit and H2B-Ub and H2B along the Cyclin B2 promoter after infections with control GFP Adenovirus (black bars) or with the YA-DN (light gray bars). Cells were arrested in G2/M by nocodazole treatment and nucleosomes were analyzed with the appropriate amplicons. The G2/M gene CDC2 and the housekeeping SON were analyzed in the core promoter and in the transcribed area (+400) (Top Right). Note the increase in H2B levels in the core promoter area upon NF-Y eviction. No H2B increase was observed in G1/S genes not expressed in G2/M cells, such as CyclinD1 (CCND1), E2F1, PCNA, CyclinA2 (CCNA2) and TOPO II α) and tissue-specific genes (MYO and AIRE) not expressed in HCT116 cells (Bottom Right).

(B) NF-YB was inactivated with shRNA produced by infections with a lentivirus (light gray bars), and compared with a Scramble shRNA control (black bars). Cells were treated and MNase I ChIPs performed as illustrated above. The CyclinB2 nucleosomes are indicated. ChIPs were performed with the indicated antibodies and analyzed by qPCR. (Left) Western blots of NF-YB in the control and NF-YB shRNA treated cells. Data are presented as mean ± SD. The results are from three biological replicates, and each quantitative PCR was performed in triplicate.

Figure options

To assess the specific role of Lys138(YB), we prepared a Flag-NF-YB Lys138(YB)→Arg mutant to be used with NF-YC and NF-YA in transient transfections (Figure 6A). Chromatin from cells in which the wild-type (WT) or Lys138(YB)→Arg mutant trimers were overexpressed was used in ChIPs. Figure 6B shows that WT NF-Y had positive effects on the levels of H3K4me3, H3K79me2, and H2BK120-Ub on most endogenous CCAAT promoters tested, unlike the Lys138(YB)→Arg mutant, consistent with a positive role of Lys138(YB) on the deposition of these marks. The Lys138(YB)→Arg mutant does not impair DNA binding of the trimer: ChIPs with anti-Flag antibodies indicated that Flag-NF-YB, WT or Lys138(YB)→Arg, was found with similar efficiencies on CCAAT promoters (Figure 6B, bottom). Histone PTM levels on the CCAAT-less C/EBPβ, and their overall levels, as verified by WBs (Figure 6A), were not modified. We then evaluated the transcriptional effect of the mutant on many endogenous CCAAT genes by quantitative reverse-transcription PCR: Figure 6C shows that in 21 of 33 promoters, there was a 2- to 4-fold dominant-negative effect; in 8 there was an increase in expression with the WT trimer, but not with the Lys138(YB)→Arg mutant; and in only 2 (RAD17 and ANK54), WT and mutant behaved similarly. CCAAT-less genes were unaffected. In conclusion, Lys138(YB) plays an important role in NF-Y transcriptional activation by allowing the deposition of H3 methylations (Dolfini et al., 2012) as well as H2B ubiquitination.

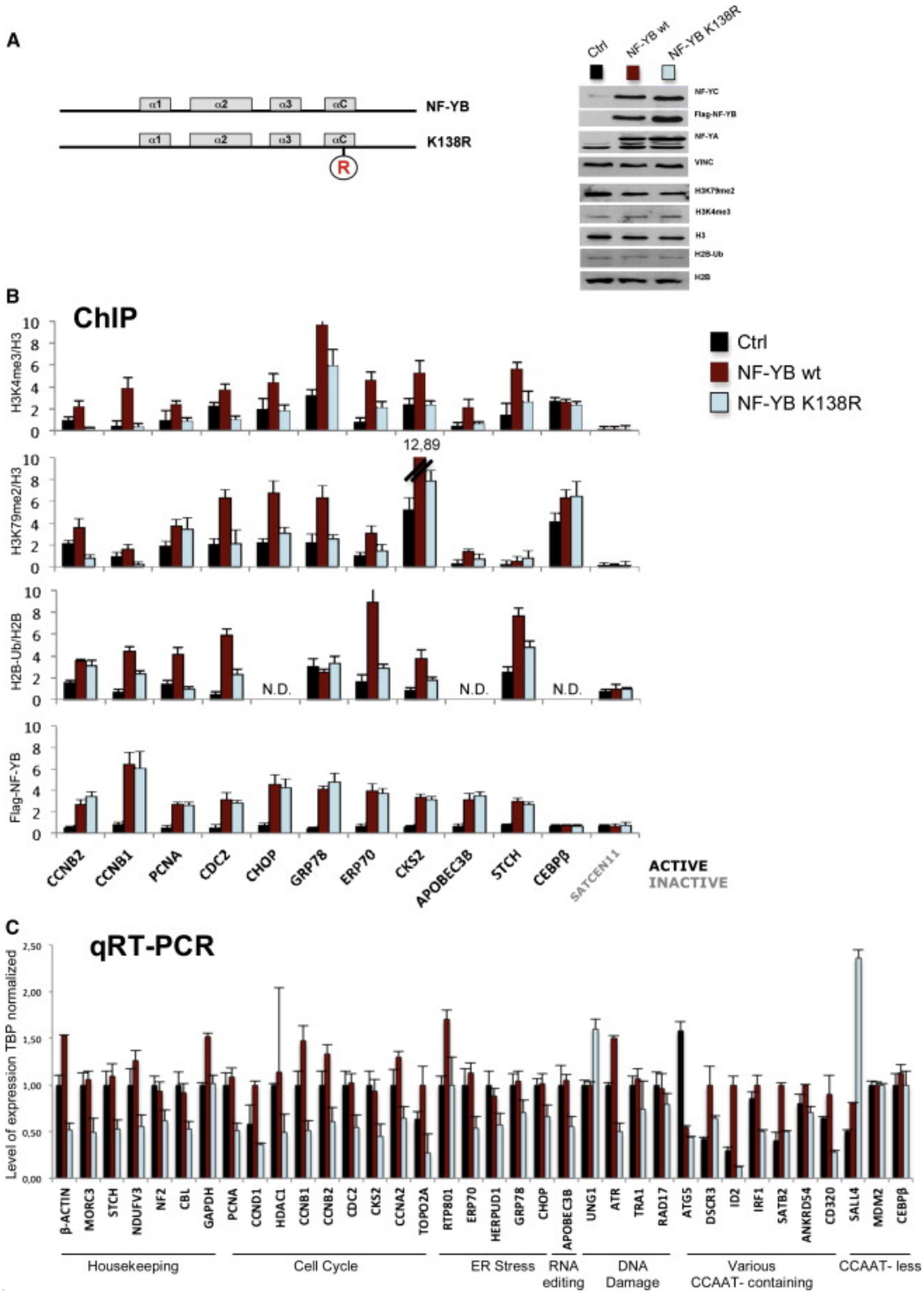

Figure 6.

The Lys138(YB)→Arg Mutant Is Defective in Deposition of H2BK120-Ub, H3K4me3, and H3K79me2 and Transcriptional Activation of CCAAT Promoters

(A) Flag-NF-YB (WT and the Lys138(YB)→Arg mutant) used for transient transfection in HCT116 cells, together with NF-YA and NF-YC-expressing plasmids. Overexpressed proteins were monitored by western blotting (right). Ctrl, control.

(B) ChIP analysis was done on the indicated CCAAT promoters with H3K79me, H3K4me3, and H2BK120-Ub antibodies. Fold enrichments over a control antibody, normalized for H3 or H2B levels, are indicated. (Bottom) ChIPs were performed with an anti-Flag antibody. The CCAAT-less C/EBPβ and Satellite DNA are controls. Mock-transfected cells are indicated by black bars, WT NF-Y trimer by red bars, and NF-Y trimer bearing the Lys138(YB)→Arg mutation by light-blue bars, respectively. Black or gray labels denote gene activity (active or inactive, respectively). N.D., not detectable.

(C) Transient transfection as above: quantitative reverse-transcription PCR analysis of expression of different types of CCAAT-dependent genes was performed on cells mock transfected with WT NF-Y trimer or with NF-Y Lys138(YB)→Arg mutant trimer. The CCAAT-less MDM2 and C/EBPβ were used as controls. The expression data were normalized for TBP mRNA expression, also produced from a CCAAT-less gene. Data are presented as mean ± SD. The results are from three biological replicates, and each quantitative PCR was performed in triplicate.

See also Figure S5.

Figure options

Finally, we checked the NF-YB ubiquitination status in vivo. We performed re-ChIP assays with NF-YB, H2B, and the anti-Ub antibodies (Figure 7). In the G2/M cell setup employed above, there was an enrichment of NF-Y and NF-Y/Ub on the active CyclinB2, CDC2, and SON promoters, but not on the inactive G1/S PCNA. H2BK120-Ub was indeed positive on the transcribed regions of active genes, as expected. Altogether, these data indicate that NF-YB is indeed ubiquitinated in vivo on active promoters.

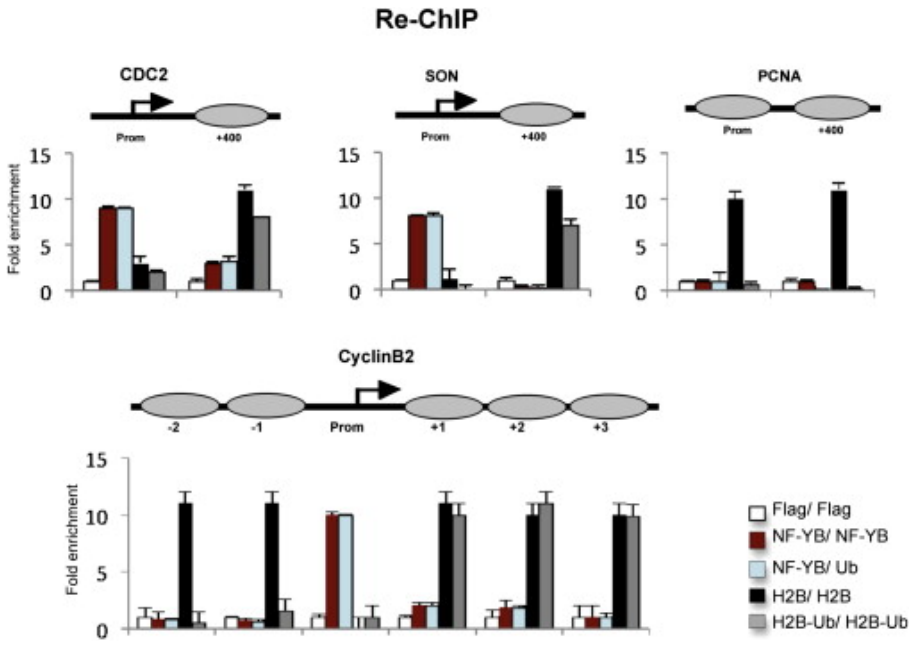

Figure 7.

NF-YB-Ub on Active CCAAT Promoters In Vivo

Re-ChIP analysis of MNase I-treated chromatin from synchronized (G2/M) HCT116 cells. The first and second antibodies sequentially used in re-ChIPs are indicated. The position of the amplicons with respect to TSS is indicated. Data are presented as mean ± SD. The

results are from three biological replicates, and each quantitative PCR was performed in triplicate.

Figure options

Discussion

This study on NF-Y highlights two main results that bring new concepts into the DNA recognition and epigenetics fields: (1) the 3D structure of the NF-Y/CCAAT complex clearly depicts a "deviant" H2A/H2B-like histone dimer (NF-YB/NF-YC) that marks transcription units thanks to a so far undisclosed sequence recognition module (NF-YA); and (2) the H2B-like NF-YB subunit is ubiquitinated at the conserved Lys138(YB), and this modification is essential for transcriptional activation, indeed a prerequisite for H2BK120-Ub and crucial H3 methylations.

NF-YA Sequence-Specific Binding

Core and variant histones form tight, yet dynamic contacts with genomic DNA within nucleosomes. In general, whereas in vitro and in vivo data provide evidence for some sequence preference in nucleosome positioning, histones are lacking discernible sequence specificity. Based on the DNA contacts here reported, the NF-YB/NF-YC HFD dimer is no exception to this rule, but the presence of NF-YA provides sequence recognition capability by means of a relatively small protein segment. The A1 helix (mostly positively charged) of NF-YA must first bind to a composite crevice (mostly negatively charged) centered on NF-YC αC in the HFD dimer (Figures 1 and 2B), a structural feature that clearly deviated from H2A/H2B (Figures 2C and S1B). As a result, NF-Y conjugates the HFD capacity to form stable but aspecific complexes with DNA, with sequence specificity that targets it to key functional locations. NF-YA is apparently the limiting subunit of the trimer, considering that HFD subunits are more abundant in vivo (Dolfini et al., 2012). Binding may be initiated by nonspecific HFD interactions with DNA, with NF-YA A1 interacting with the HFD dimer, and the interhelical A1A2 linker being instrumental in allowing the A2 helix to "search" for a CCAAT box, thus fixing binding in a stable complex. The high number (41) and nature of protein/DNA contacts fully explain the very high affinity and specificity of the complex (Figure 1C).

Our structural results reveal the unique DNA-reading mode exploited by the NF-YA subunit, based on the insertion of the A2 helix in the DNA minor groove and the presence of a conserved GxGGRF motif in the following loop (Figures 1 and 3). Such minor groove interaction is one of the most remarkable features in the NF-Y/CCAAT complex because it provides a means to induce a significant bend in the DNA, precisely between C and A of CCAAT. Most importantly, this also allows, and possibly promotes, binding in the adjacent major grooves of other TFs, whose recognition sequences are thus left accessible.

The NF-YA DNA-binding motif resembles the CCT domain of *Arabidopsis thaliana* COSTANS (Figure S3), a protein belonging to a large family of crucial regulators of plant flowering (Wenkel et al., 2006). CO binds to members of the large NF-YB/NF-YC plant families, and the interaction is physiologically relevant: mutants in At-*NF-YB/NF-YC* phenocopy the *co* mutants, in terms of delayed flowering-time phenotype (Ben-Naim et al., 2006; Cai et al., 2007; Chen et al., 2007; Kumimoto et al., 2010). At-NF-YA1 overexpression causes late flowering, suggesting that CO and At-NF-YAs might compete for the occupancy of At-NF-YB/NF-YC dimers (Wenkel et al., 2006). We observe that mutations affecting CO activity in vivo (Wenkel et al., 2006) match the position of amino acids essential for DNA binding by NF-YA (Figure S3). Thus, our results open an entirely new framework for structural and functional characterization of the CO/At-NF-Y interplay.

The NF-YB/NF-YC HFD Dimeric Module

The 3D structure proves that NF-Y contacts DNA through its deviant HFD module in a manner almost identical to that of core histones within the nucleosome, particularly related to their conserved structural and electrostatic complementarity to DNA (Figures 2C and 4A). The complex provides structural clues that extend to related HFD proteins, in particular to NC2α/β. NC2 acts negatively on TATA (Kamada et al., 2001) and positively on Downstream Promoter Elements that lie at +25 bp from the TSS (Hsu et al., 2008). DNA binding coded by TBP is instrumental for stabilization of the NC2α/β with TATA. The HFD modules of NF-Y and NC2 are very similar in terms of 3D structure and sequence (Figures 4B and S1B), and neither NF-YB/NF-YC nor NC2α/β dimers associate to DNA in vitro in the absence of their partners (NF-YA and TBP, respectively). Such similarity extends further because NF-YA mediates DNA binding and bending by inserting residue Phe289 into the minor groove (between C and A in the CCAAT box) similarly to TBP, whose residues Phe284 and Phe193 insert into the first and last base pairs of the targeted sequence, respectively, kinking twice the DNA (Figure 3). Thus, in NF-Y and, presumably, in NC2α/β/TBP complexes, overall DNA bending induced by the nonspecific HFD-DNA interactions is further increased locally by insertion of the "DNA-reading" subunit.

These considerations bear structural implications for other H2A/H2B-like proteins, such as Chrac-17 (POLE3)/Chrac-15, associated to the remodeling complex ACF1/ISWI (Kukimoto et al., 2004; Corona et al., 2000), NC2β, associated to YEATS2 in ATAC complexes (Suganuma et al., 2008; Wang et al., 2008), and Chrac-17 (Dpb4)/Dpb3, in the DNA polymerase ε (Li et al., 2000). According to the NF-Y/CCAAT model, such HFD proteins may contact DNA in similar fashions because residues building the positively charged DNA-contacting interface are generally mostly conserved (Figures 2C and S1B). It remains to be seen whether similar considerations could extend to the TAF4/TAF12 subunits of TFIID (Figure 2C), shown to hold DNA binding directed at subclasses of core promoters (Wright et al., 2006; Gazit et al., 2009).

An Extension of the Transtail Model

H2B monoubiquitination is an early event in gene activation, with genetic and biochemical links to H3K4me3, H3K79me2 deposition, and to RNA Pol II elongation, because it is predominantly found in transcribed areas of genes (Minsky et al., 2008; Batta et al., 2011). Our findings point at a common pathway of monoubiquitination conserved from NF-Y (at Lys138(YB)) to H2B (at Lys120), delineating a sequence-specific version of the current H2B-based model restricted to promoters with a CCAAT box. How ubiquitination and methylation complexes and, in general, epigenetic marks are recruited in a correct spatiotemporal way on specific locations of genomes is a key question. Our functional experiments establish an order of priorities concerning a sizeable class of promoters in which NF-Y binding is one of the earliest events. The identification of an HFD-mediated monoubiquitination pathway, which is promoter (CCAAT) specific, strongly suggests that, beyond structural relationships, the similarities between core and "deviant" histones are also functional, providing a further layer of potential epigenetic control. The literature is in no shortage of examples of interplay between NF-Y and specific TFs, shown to require prior NF-Y binding, and indeed a specific precise distance of sites, for synergistic function (Dolfini et al., 2009). Many TFs require the presence of histone PTMs, notably methylations: one can imagine that either during DNA replication, when some preinitiation complexes (PICs) are established, or possibly during de novo assembly of PICs, NF-Y could prevent nucleosome formation in specific locations, recruiting histone-modifying machines and providing space for TFs to bind nearby. Indeed, studies of nucleosome positioning in yeast placed CCAAT in the top list of "open" TF-binding sites (Segal et al., 2006). Considering this, our data suggest that NF-Y plays a pioneer role in the establishment of active promoters.

Several important questions are lying ahead: one concerns the nature of the NF-YB monoubiquitination apparatus, which is unknown; a second regards the presence of NF-YB PTMs similar to those detected in H2B, other than Lys138(YB) and H2B Lys120 monoubiquitination. H2B, in fact, displays PTMs that are not only localized in tails, but also within the HFD (Cosgrove et al., 2004): H2BK43me and H2BK85ac, for example, affect residues that are conserved in their nature and locations in NF-YB (Lys67 and Lys107, respectively). Indeed, NF-YB is acetylated, by p300/CBP and Gcn5/PCAF, and interacts with SAGA (Dolfini et al., 2012). It will thus be important to determine which are the targeted NF-YB Lys residues and what is the functional effect of such modifications. Finally, opposite to H2BK120-Ub, H2A monoubiquitination has the functional significance of Polycomb-mediated transcriptional repression: because evidence for a role of NF-Y in active repression, both at single sites and at the genomic level, is piling up (Dolfini et al., 2012), the ensuing question is whether this is exerted via NF-YC ubiquitination. In this scenario, NF-Y would be neither an activator nor a repressor per se but rather a bookmark of genomic regions to be switched on or off with epigenetic signals.

In conclusion, the data here presented for the NF-Y/CCAAT complex fully detail the DNA recognition mode of this sequence-specific TF containing a deviant histone dimer and identify a NF-YB posttranslational modification required to set up a positive chromatin configuration in CCAAT promoters. These results provide a fundamental platform for further mechanistic analyses on the formation of larger complexes with nearby TFs, coactivators, and the general Pol II machinery.

Experimental Procedures

Protein Expression, Purification, Crystallization, Data Collection, Structure Determination, and Refinement

The NF-Y complex was purified exploiting the coexpression system described in Diebold et al. (2011), and after addition of the 25 bp CCAAT oligo (Figure S1), the NF-Y/DNA complex was isolated by gel filtration and concentrated. Crystals were grown by the hanging-drop vapor diffusion method using as precipitant solution 20%–24% PEG3350, 100 mM Mes or Cacodylate buffer (pH 6.5), and 50 mM NaF, at 20°C. NF-Y/DNA crystals diffracted to 3.1 Å resolution at the ESRF synchrotron (ID29 beamline; Grenoble, France) and belong to the space group $P2_12_12_1$, with one NF-Y/DNA complex per asymmetric unit. Raw data were processed with XDS and Scala (Kabsch, 2010; Evans, 2006). The structure was solved by a composite molecular replacement approach based on Phaser (Storoni et al., 2004), using the NF-YB/NF-YC coordinates (PDB 1N1J) as the search model for the protein part of the complex, whereas a 25 bp oligonucleotide from the *X. laevis* nucleosome (PDB 1AOI) was used for the DNA component. The two independent solutions were combined into a unique protein-DNA model and refined as rigid bodies using Refmac (Murshudov et al., 1997). The oligonucleotide sequence was then model built into the DNA electron density using Coot (Emsley and Cowtan, 2004). Improvement of the electron density quality was achieved following TLS-restrained refinement with BUSTER (Bricogne et al., 2010), using LSSR restraints to the 1N1J model, allowing identification and model building of the NF-YA subunit structure. The final model was restrain refined with TLS at 3.1 Å (R_{work} = 0.19, R_{free} = 0.25) using Refmac (Murshudov et al., 1997) (Table S1). A sample of protein and DNA electron density is shown in Figure S2. Details for protein complex expression, purification, and crystallization are in the Extended Experimental Procedures.

NF-YB Mutant Expression Vectors

Lysine-to-Arginine total mutant NF-YB-K-all-R was generated on the backbone of the NF-YB-Flag expression vector with the QuikChange Multi Site-Directed Mutagenesis Kit (Stratagene) by consecutive mutagenesis (see Extended Experimental Procedures). Single lysines were reintroduced in the NF-YB-K-all-R by site-specific mutagenesis with appropriate oligos for the selected residues.

Immunoprecipitation-WB Analyses

For detection of mono-ubiquitination of endogenous NF-YB, NIH 3T3 nuclear extracts (1 mg) were immunoprecipitated with anti-NF-YB (30 μg), or anti-TRX as a control. The eluted material was run on WBs and probed with anti-Ubiquitin (PW8810; Biomol). For the isolation of WT or mutant Flag-NF-YB, immunoprecipitation was performed from total extracts of Cos-1-transfected cells (250 μg), with 5 μg of anti-NF-YB antibodies.

ChIP and Re-ChIP

ChIP and MNaseI ChIP assays were performed as previously described (Gatta and Mantovani, 2010) with 3–5 μg of the relevant antibodies, indicated in Extended Experimental Procedures. For re-ChIP assay, IP-enriched DNAs were eluted in 1% SDS, 50 mM $NaHCO_3$, for 30 min at 35°C, and diluted 1:10 with IP buffer (50 mM Tris-HCl [pH 8], 10 mM EDTA, 0.1% SDS, 0.5% deoxycholic acid, 150 mM LiCl, and protease inhibitors) to perform the second IP.

Extended Experimental Procedures

Acknowledgments

M.N., N.G., G.D., R.G., C.F., and A.F. performed the experiments; M.N. and C.V. analyzed the X-ray data; and M.N., N.G., D.M., C.R., M.B., and R.M. planned the experiments, analyzed the data, and wrote the manuscript. We thank David Horner for comments on the manuscript. This work was supported by Regione Lombardia Nepente grant (to R.M.), and by institutional funds from the CNRS, INSERM, the Université de Strasbourg (UDS), and the European Commission SPINE2-Complexes project (contract No. LSHG-CT-2006-031220).

Accession Numbers

Atomic coordinates have been deposited in the RCSB Protein Data Bank under ID code 4AWL.

Document S2. Article plus Supplemental Information.

Help with PDF files
Options

References

- K. Batta, Z. Zhang, K. Yen, D.B. Goffman, B.F. Pugh Genome-wide function of H2B ubiquitylation in promoter and genic regions Genes Dev., 25 (2011), pp. 2254–2265

- O. Ben-Naim, R. Eshed, A. Parnis, P. Teper-Bamnolker, A. Shalit, G. Coupland, A. Samach, E. Lifschitz The CCAAT binding factor can mediate interactions between CONSTANS-like proteins and DNA Plant J., 46 (2006), pp. 462–476
- W. Bi, L. Wu, F. Coustry, B. de Crombrugghe, S.N. Maity DNA binding specificity of the CCAAT-binding factor CBF/NF-Y J. Biol. Chem., 272 (1997), pp. 26562–26572
- G. Bricogne, E. Blanc, M. Brandl, C. Flensburg, P. Keller, W. Paciorek, P. Roversi, A. Sharff, O.S. Smart, C. Vonrhein, T.O. Womack BUSTER version 2.9 Global Phasing, Cambridge (2010)
- X. Cai, J. Ballif, S. Endo, E. Davis, M. Liang, D. Chen, D. DeWald, J. Kreps, T. Zhu, Y. Wu A putative CCAAT-binding transcription factor is a regulator of flowering timing in *Arabidopsis* Plant Physiol., 145 (2007), pp. 98–105
- N.Z. Chen, X.Q. Zhang, P.C. Wei, Q.J. Chen, F. Ren, J. Chen, X.C. Wang AtHAP3b plays a crucial role in the regulation of flowering time in *Arabidopsis* during osmotic stress J. Biochem. Mol. Biol., 40 (2007), pp. 1083–1089
- D.F. Corona, A. Eberharter, A. Budde, R. Deuring, S. Ferrari, P. Varga-Weisz, M. Wilm, J. Tamkun, P.B. BeckerTwo histone fold proteins, CHRAC-14 and CHRAC-16, are developmentally regulated subunits of chromatin accessibility complex (CHRAC) EMBO J., 19 (2000), pp. 3049–3059
- M.S. Cosgrove, J.D. Boeke, C. Wolberger Regulated nucleosome mobility and the histone code Nat. Struct. Mol. Biol., 11 (2004), pp. 1037–1043
- M.L. Diebold, S. Fribourg, M. Koch, T. Metzger, C. Romier Deciphering correct strategies for multiprotein complex assembly by co-expression: application to complexes as large as the histone octamer J. Struct. Biol., 175 (2011), pp. 178–188
- D. Dolfini, F. Zambelli, G. Pavesi, R. Mantovani A perspective of promoter architecture from the CCAAT box Cell Cycle, 8 (2009), pp. 4127–4137
- D. Dolfini, R. Gatta, R. Mantovani NF-Y and the transcriptional activation of CCAAT promoters Crit. Rev. Biochem. Mol. Biol., 47 (2012), pp. 29–49
- P. Emsley, K. Cowtan Coot: model-building tools for molecular graphics Acta Crystallogr. D Biol. Crystallogr., 60 (2004), pp. 2126–2132
- J. Ernst, P. Kheradpour, T.S. Mikkelsen, N. Shoresh, L.D. Ward, C.B. Epstein, X. Zhang, L. Wang, R. Issner, M. Coyne, *et al.* Mapping and analysis of chromatin state dynamics in nine human cell types Nature, 473 (2011), pp. 43–49
- P. Evans Scaling and assessment of data quality Acta Crystallogr. D Biol. Crystallogr., 62 (2006), pp. 72–82
- Y.G. Gangloff, C. Romier, S. Thuault, S. Werten, I. Davidson The histone fold is a key structural motif of transcription factor TFIID Trends Biochem. Sci., 26 (2001), pp. 250–257
- R. Gatta, R. Mantovani Single nucleosome ChIPs identify an extensive switch of acetyl marks on cell cycle promoters Cell Cycle, 9 (2010), pp. 2149–2159
- K. Gazit, S. Moshonov, R. Elfakess, M. Sharon, G. Mengus, I. Davidson, R. Dikstein TAF4/4b x TAF12 displays a unique mode of DNA binding and is required for core promoter function of a subset of genes J. Biol. Chem., 284 (2009), pp. 26286–26296
- K.F. Hartlepp, C. Fernández-Tornero, A. Eberharter, T. Grüne, C.W. Müller, P.B. Becker The histone fold subunits of *Drosophila* CHRAC facilitate nucleosome sliding through dynamic DNA interactions Mol. Cell. Biol., 25 (2005), pp. 9886–9896
- J.Y. Hsu, T. Juven-Gershon, M.T. Marr II, K.J. Wright, R. Tjian, J.T. Kadonaga TBP, Mot1, and NC2 establish a regulatory circuit that controls DPE-dependent versus TATA-dependent transcription Genes Dev., 22 (2008), pp. 2353–2358
- Z.S. Juo, T.K. Chiu, P.M. Leiberman, I. Baikalov, A.J. Berk, R.E. Dickerson How proteins recognize the TATA box J. Mol. Biol., 261 (1996), pp. 239–254
- W. Kabsch XDS Acta Crystallogr. D Biol. Crystallogr., 66 (2010), pp. 125–132

- K. Kamada, F. Shu, H. Chen, S. Malik, G. Stelzer, R.G. Roeder, M. Meisterernst, S.K. Burley
- Crystal structure of negative cofactor 2 recognizing the TBP-DNA transcription complex Cell, 106 (2001), pp. 71–81
- J.L. Kim, D.B. Nikolov, S.K. Burley Co-crystal structure of TBP recognizing the minor groove of a TATA element Nature, 365 (1993), pp. 520–527
- Kukimoto, S. Elderkin, M. Grimaldi, T. Oelgeschläger, P.D. Varga-Weisz The histone-fold protein complex CHRAC-15/17 enhances nucleosome sliding and assembly mediated by ACF Mol. Cell, 13 (2004), pp. 265–277
- R.W. Kumimoto, Y. Zhang, N. Siefers, B.F. Holt 3rd NF-YC3, NF-YC4 and NF-YC9 are required for CONSTANS-mediated, photoperiod-dependent flowering in *Arabidopsis thaliana* Plant J., 63 (2010), pp. 379–391
- R.N. Laribee, S.M. Fuchs, B.D. Strahl H2B ubiquitylation in transcriptional control: a FACT-finding mission Genes Dev., 21 (2007), pp. 737–743
- Q. Li, M. Herrler, N. Landsberger, N. Kaludov, V.V. Ogryzko, Y. Nakatani, A.P. Wolffe *Xenopus* NF-Y pre-sets chromatin to potentiate p300 and acetylation-responsive transcription from the *Xenopus* hsp70 promoter in vivo EMBO J., 17 (1998), pp. 6300–6315
- Y. Li, Z.F. Pursell, S. Linn Identification and cloning of two histone fold motif-containing subunits of HeLa DNA polymerase epsilon J. Biol. Chem., 275 (2000), pp. 23247–23252
- C. Liberati, A. di Silvio, S. Ottolenghi, R. Mantovani NF-Y binding to twin CCAAT boxes: role of Q-rich domains and histone fold helices J. Mol. Biol., 285 (1999), pp. 1441–1455
- K. Luger, A.W. Mäder, R.K. Richmond, D.F. Sargent, T.J. Richmond Crystal structure of the nucleosome core particle at 2.8 A resolution Nature, 389 (1997), pp. 251–260
- N. Minsky, E. Shema, Y. Field, M. Schuster, E. Segal, M. Oren Monoubiquitinated H2B is associated with the transcribed region of highly expressed genes in human cells Nat. Cell Biol., 10 (2008), pp. 483–488
- G.N. Murshudov, A.A. Vagin, E.J. Dodson Refinement of macromolecular structures by the maximum-likelihood method Acta Crystallogr. D Biol. Crystallogr., 53 (1997), pp. 240–255
- Z. Nagy, L. Tora Distinct GCN5/PCAF-containing complexes function as co-activators and are involved in transcription factor and global histone acetylation Oncogene, 26 (2007), pp. 5341–5357
- R.A. Poot, G. Dellaire, B.B. Hülsmann, M.A. Grimaldi, D.F. Corona, P.B. Becker, W.A. Bickmore, P.D. Varga-Weisz HuCHRAC, a human ISWI chromatin remodelling complex contains hACF1 and two novel histone-fold proteins EMBO J., 19 (2000), pp. 3377–3387
- K. Robzyk, J. Recht, M.A. Osley Rad6-dependent ubiquitination of histone H2B in yeast Science, 287 (2000), pp. 501–504
- C. Romier, F. Cocchiarella, R. Mantovani, D. Moras The NF-YB/NF-YC structure gives insight into DNA binding and transcription regulation by CCAAT factor NF-Y J. Biol. Chem., 278 (2003), pp. 1336–1345
- Ronchi, M. Bellorini, N. Mongelli, R. Mantovani CCAAT-box binding protein NF-Y (CBF, CP1) recognizes the minor groove and distorts DNA Nucleic Acids Res., 23 (1995), pp. 4565–4572
- A.J. Ruthenburg, C.D. Allis, J. Wysocka Methylation of lysine 4 on histone H3: intricacy of writing and reading a single epigenetic mark Mol. Cell, 25 (2007), pp. 15–30
- E. Segal, Y. Fondufe-Mittendorf, L. Chen, A. Thåström, Y. Field, I.K. Moore, J.P. Wang, J. Widom A genomic code for nucleosome positioning Nature, 442 (2006), pp. 772–778
- L.C. Storoni, A.J. McCoy, R.J. Read Likelihood-enhanced fast rotation functions Acta Crystallogr. D Biol. Crystallogr., 60 (2004), pp. 432–438
- T. Suganuma, J.L. Workman Signals and combinatorial functions of histone modifications Annu. Rev. Biochem., 80 (2011), pp. 473–499

- T. Suganuma, J.L. Gutiérrez, B. Li, L. Florens, S.K. Swanson, M.P. Washburn, S.M. Abmayr, J.L. Workman ATAC is a double histone acetyltransferase complex that stimulates nucleosome sliding Nat. Struct. Mol. Biol., 15 (2008), pp. 364–372
- S.A. Wagner, P. Beli, B.T. Weinert, M.L. Nielsen, J. Cox, M. Mann, C. Choudhary A proteome-wide, quantitative survey of in vivo ubiquitylation sites reveals widespread regulatory roles Mol. Cell. Proteomics, 10 (2011) M111.013284
- Y.L. Wang, F. Faiola, M. Xu, S. Pan, E. Martinez Human ATAC Is a GCN5/PCAF-containing acetylase complex with a novel NC2-like histone fold module that interacts with the TATA-binding protein J. Biol. Chem., 283 (2008), pp. 33808–33815
- V.M. Weake, J.L. Workman Histone ubiquitination: triggering gene activity Mol. Cell, 29 (2008), pp. 653–663
- S. Wenkel, F. Turck, K. Singer, L. Gissot, J. Le Gourrierec, A. Samach, G. Coupland CONSTANS and the CCAAT box binding complex share a functionally important domain and interact to regulate flowering of *Arabidopsis* Plant Cell, 18 (2006), pp. 2971–2984
- S. Werten, A. Mitschler, C. Romier, Y.G. Gangloff, S. Thuault, I. Davidson, D. Moras Crystal structure of a subcomplex of human transcription factor TFIID formed by TATA binding protein-associated factors hTAF4 (hTAF(II)135) and hTAF12 (hTAF(II)20) J. Biol. Chem., 277 (2002), pp. 45502–45509
- K.J. Wright, M.T. Marr II, R. Tjian TAF4 nucleates a core subcomplex of TFIID and mediates activated transcription from a TATA-less promoter Proc. Natl. Acad. Sci. USA, 103 (2006), pp. 12347–12352
- K. Zemzoumi, M. Frontini, M. Bellorini, R. Mantovani NF-Y histone fold alpha1 helices help impart CCAAT specificity J. Mol. Biol., 286 (1999), pp. 327–337

Supplemental References

- Kim, I.S., Sinha, S., de Crombrugghe, B., and Maity, S.N. (1996). Determination of functional domains in the C subunit of the CCAAT-binding factor (CBF) necessary for formation of a CBF-DNA complex: CBF-B interacts simultaneously with both the CBF-A and CBF-C subunits to form a heterotrimeric CBF molecule. Mol. Cell. Biol. *16*, 4003–4013.
-
- Laskowski, R.A., MacArthur, M.W., Moss, D.S., and Thornton, J.M. (1993). PROCHECK: a program to check the stereochemical quality of protein structure. J. Appl. Crystallogr. *26*, 283–291.
-
- Luger, K., and Richmond, T.J. (1998). DNA binding within the nucleosome core. Curr. Opin. Struct. Biol. *8*, 33–40.
-
- Maity, S.N., and de Crombrugghe, B. (1992). Biochemical analysis of the B subunit of the heteromeric CCAAT-binding factor. A DNA-binding domain and a subunit interaction domain are specified by two separate segments. J. Biol. Chem. *267*, 8286–8292.
-
- Manni, I., Caretti, G., Artuso, S., Gurtner, A., Emiliozzi, V., Sacchi, A., Mantovani, R., and Piaggio, G. (2008). Posttranslational regulation of NF-YA modulates NF-Y transcriptional activity. Mol. Biol. Cell *19*, 5203–5213.
-
- Mantovani, R., Li, X.Y., Pessara, U., Hooft van Huisjduijnen, R., Benoist, C., and Mathis, D. (1994). Dominant negative analogs of NF-YA. J. Biol. Chem. *269*, 20340–20346.

- Sinha, S., Kim, I.S., Sohn, K.Y., de Crombrugghe, B., and Maity, S.N. (1996). Three classes of mutations in the A subunit of the CCAAT-binding factor CBF delineate functional domains involved in the three-step assembly of the CBF-DNA complex. Mol. Cell. Biol. *16*, 328–337.
- Thön, M., Al Abdallah, Q., Hortschansky, P., Scharf, D.H., Eisendle, M., Haas, H., and Brakhage, A.A. (2010). The CCAAT-binding complex coordinates the oxidative stress response in eukaryotes. Nucleic Acids Res. *38*, 1098–1113.
- Xing, Y., Fikes, J.D., and Guarente, L. (1993). Mutations in yeast HAP2/HAP3 define a hybrid CCAAT box binding domain. EMBO J. *12*, 4647–4655.
- Xing, Y., Zhang, S.U., Olesen, J.T., Rich, A., and Guarente, L. (1994). Subunit interaction in the CCAAT-binding heteromeric complex is mediated by a very short alpha-helix in HAP2. Proc. Natl. Acad. Sci. USA *91*, 3009–3013.
- Zheng, G., Lu, X.J., and Olson, W.K. (2009). Web 3DNA—a web server for the analysis, reconstruction, and visualization of three-dimensional nucleic-acid structures. Nucleic Acids Res. *37*(Web Server issue), W240–W246.